The investigations of the interplanetary scintillations at decameter wavelengths: the present state and perspectives

N.N. Kalinichenko[1], A.A. Konovalenko[1], A.I. Brazhenko[2], O.L. Ivantishin[3]
O.A. Lytvynenko[1], M.R. Olyak[1], I.N. Bubnov[1], S.N. Yerin[1]

[1]Radio Astronomy institute of NAS of Ukraine
4, Mysteztv, Kharkiv, 310002, Ukraine,
kalinich@ri.kharkov.ua

[2] Gravimetrical observatory of Geophysical institute of NAS of Ukraine
27/29, Myasoedova, Poltava, 36029, Ukraine

[3] Institute of Physics and Mechanics of NAS of Ukraine,
5, Naukova, L'viv, 79060, Ukraine

Plan of report

- Observations of the interplanetary scintillations (IPS)
  at decameter wavelengths as an effective tool for the solar wind investigations.

- IPS observations in Ukraine.
  - UTR-2 and URAN system;
  - methods for data processing;
  - some results.

- Perspectives.

Interplanetary scintillations (IPS)

Hewish et al., 1964

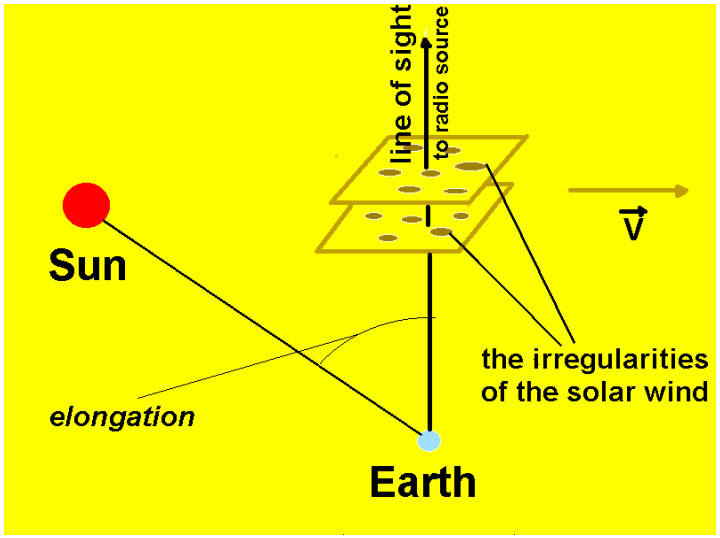

Figure 1.

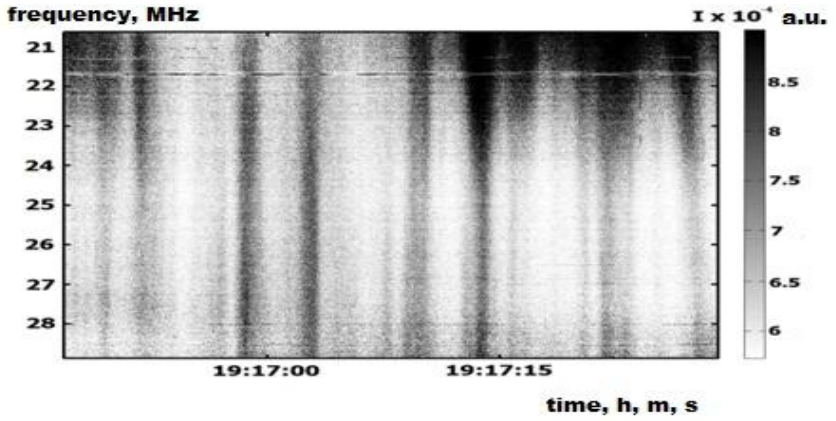

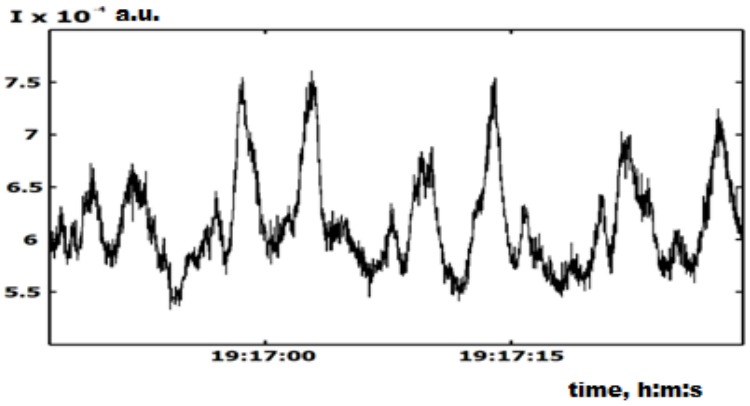

Good Points of IPS Observations are possibilities of

- **Remote sensing.**
- **Long-term monitoring**

Interplanetary scintillations at decameter wavelengths

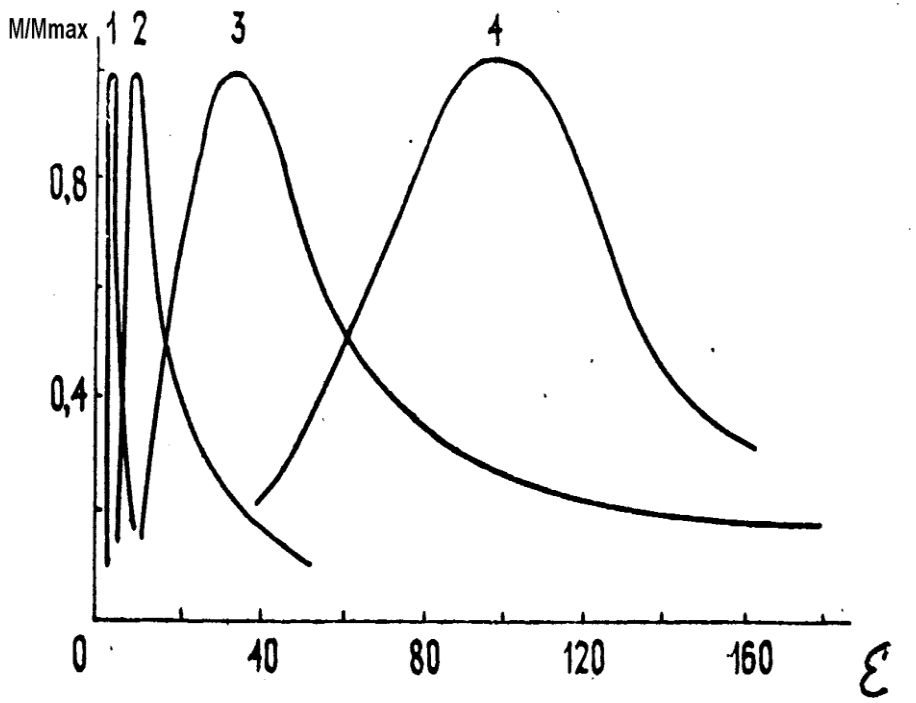

Figure 2. Dependence of normalized scintillations index m/m_m on solar elongation ε

Where:

m_m - maximum value of scintillations index.

* 1 – 2700 MHz , 3C279;

2 - 430 MHz, CTA-21;

3 - 74 MHz, 3C144;

Erskine F.T., Cronyn W.M., Shawhan S.D., Roelof E.C., Gotwols B.L. Preprint university of Iowa. N77-24. 1977. p.1.

** 4 - 25 MHz, 3C144, UTR-2 .

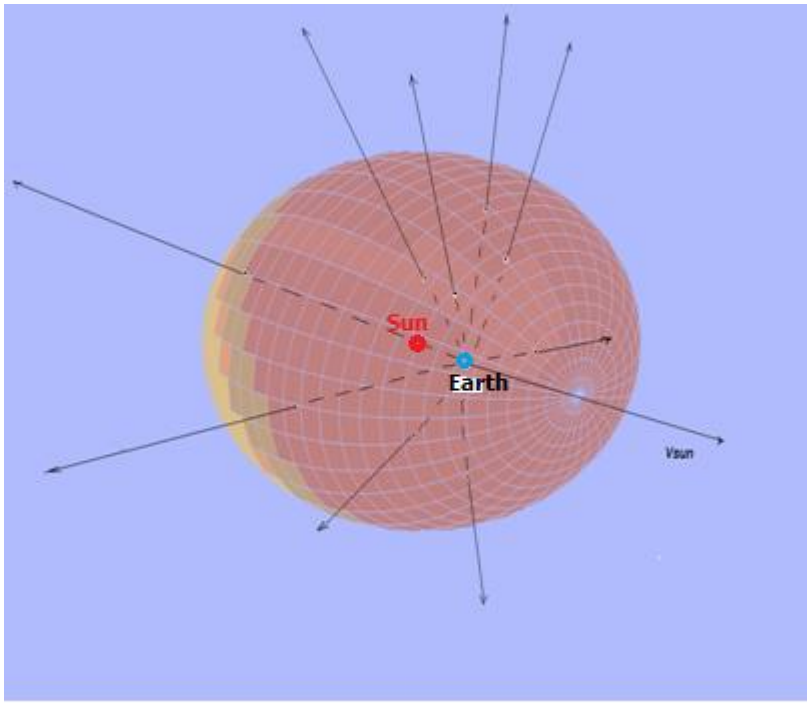

Figure 3. Decameter range of radio waves provides a real global coverage of the inner heliosphere up to several AU.

Our investigations briefly consist of:

- Observations of IPS.
- Theoretical investigations and modeling of IPS.
- Fitting the theoretical model to the observed IPS characteristics.

Observations.
Outward appearances of
Ukrainian decameter radio telescopes for interplanetary and ionospheric scintillation observations

UTR-2, 8 – 32 MHz (Kharkiv)

URAN-2, 8 – 32 MHz (Poltava)

URAN-4, 8 – 32 MHz (Odesa)

URAN- 1, 8 – 32 MHz (Zmiev)

URAN- 3, 8 – 32 MHz (Lviv)

GURT, 8 – 80 MHz (Kharkiv)

Figure 4.

Examples of IPS at decameter wavelengths at different elongations (small, large and very small)

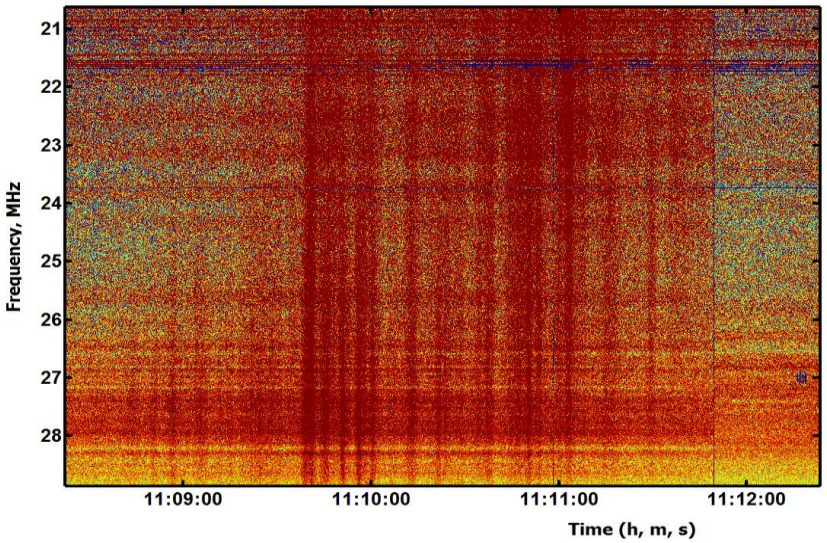

Figure 6. Dynamic spectrum of interplanetary scintillations at a small elongation (40 degree).
(Radio telescope UTR-2. Radio source 4C21.53 associated with a pulsar)

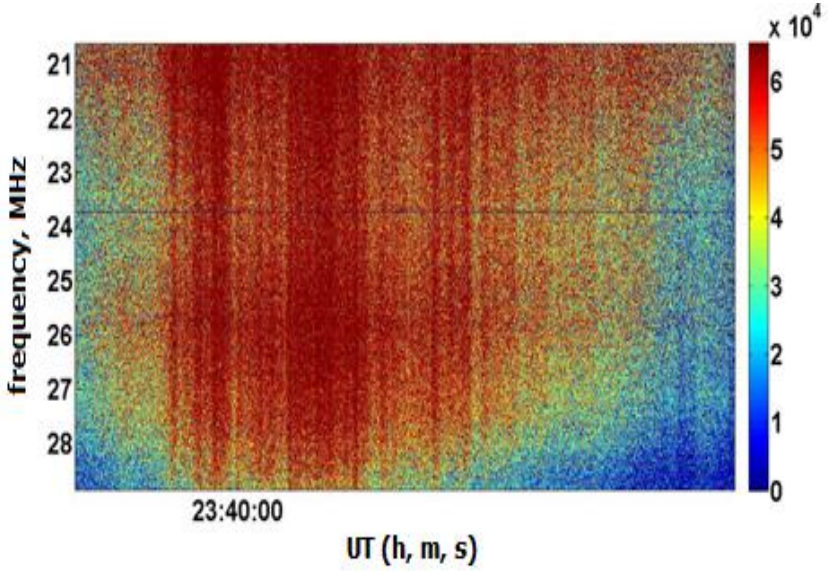

Figure 7. Dynamic spectrum of interplanetary scintillations at a large elongation (170 degree).
(Radio telescope UTR-2. Radio source 3C196 associated with a quasar)

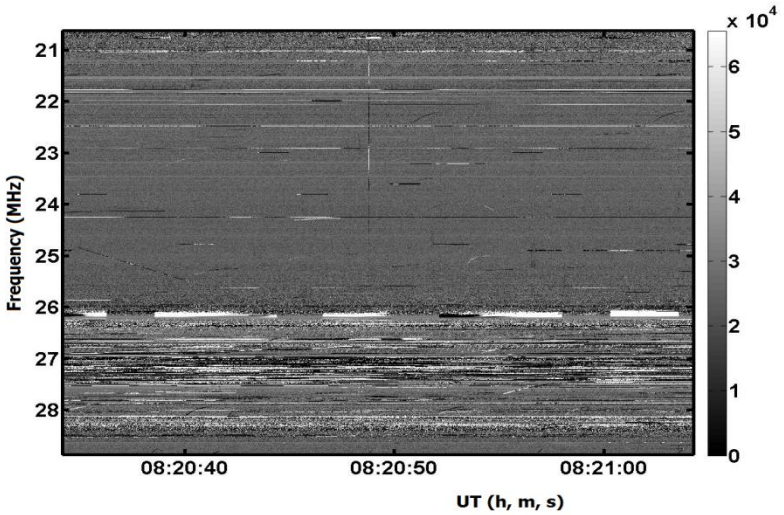

Figure 8. Observations of radio source 3C144 at very small elongation (8 degrees). There are no interplanetary scintillations.

Kalinichenko et al., 2012

Harmful effects

- relatively high level of interference, especially at day time.
- ionospheric effects,
- limited number of small-size decameter radio sources suitable for IPS observations.

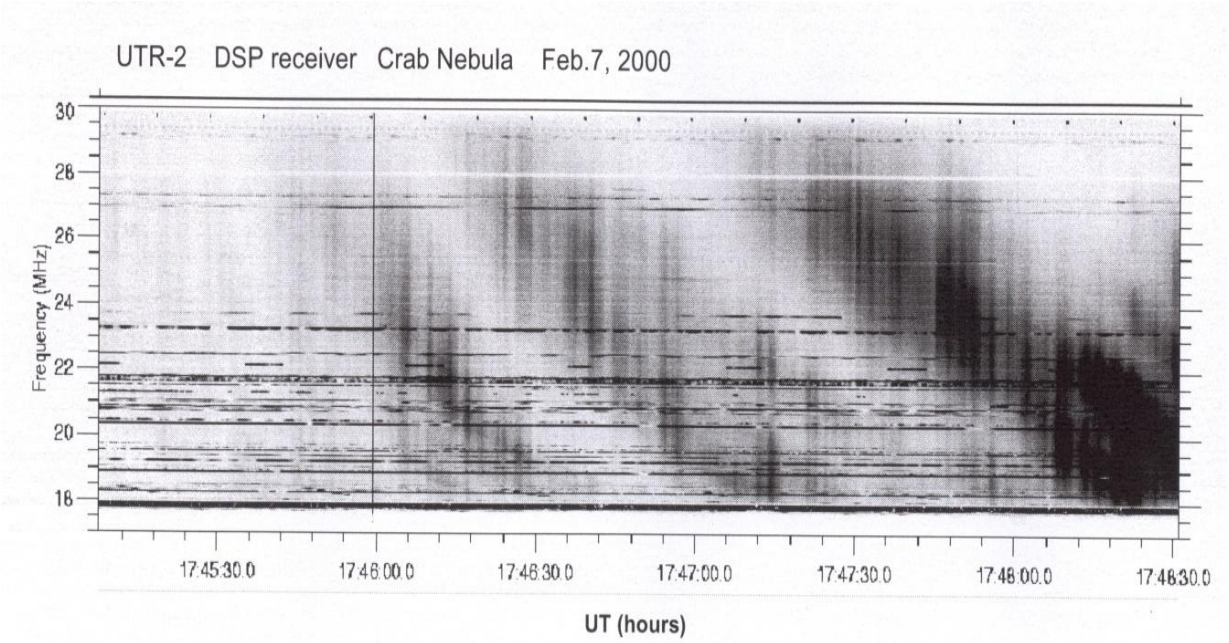

Figure 9. Dynamic spectrum of Crab Nebula scintillations.

1. Our statement is that analysis of power spectrum, spatial and frequency correlations allow to find ionospheric effect.
2. Use of DSP enables us to carry effective cleaning of IPS data from interference.

Monitoring of interplanetary medium

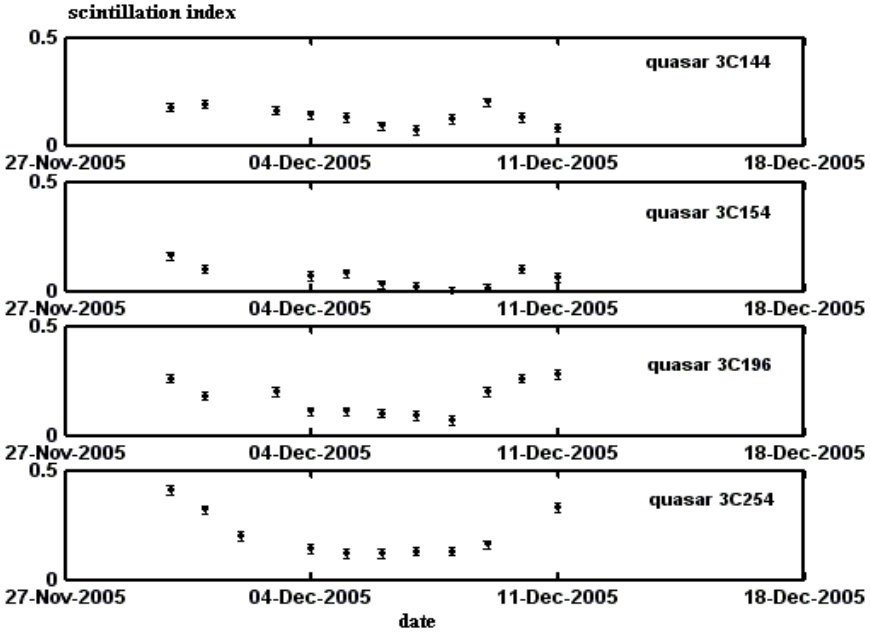

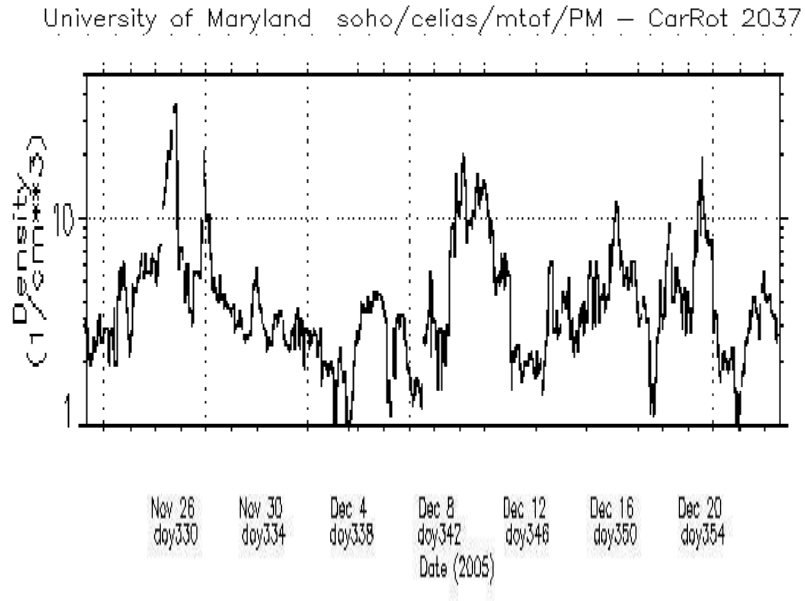

Figure 10.

Models of the solar wind

One flow model with parameters:

$$v\ ,\ \ n\ ,\sigma_N(\zeta)\ \propto\ \ R^{-b}, b\approx 2$$

where $R\equiv R(\zeta)$ is the distance from the sun

Multi-flow model including:

Slow-speed stream with parameters v_1, n_1, b_1

and one or two high-speed stream (s) with parameters

$$v_{2,3}\ ,n_{2,3}\ ,\sigma_N(\zeta)\ \propto\left[R_0+L_{2,3}\zeta\right]^{-b_{2,3}}$$

where $L_{2,3}$ is the stream thickness $0\le\zeta\le 1$ $R_0=1\text{AE}$

Spectrum analysis

The theoretical spectrum of the intensity fluctuations in one point according to Feynman path integral technique.

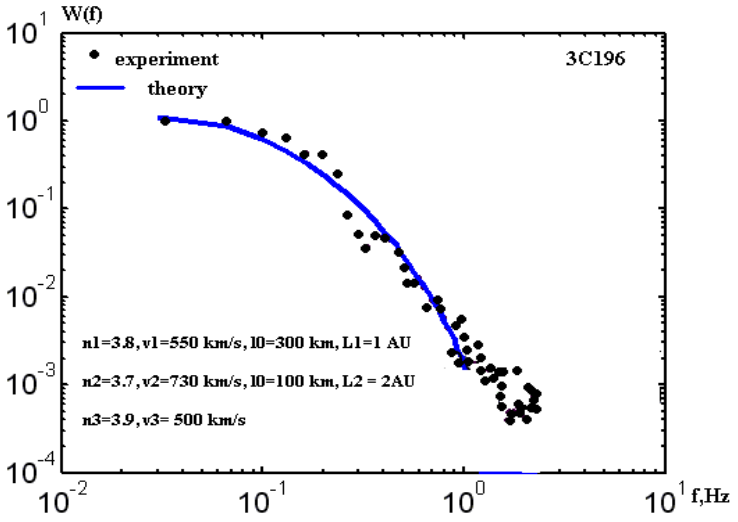

Figure 11. Example of model fitting.

$$W(f) \approx 2\pi^2 \frac{L\omega_p^4}{(c\omega)^2} \int_0^1 d\zeta \int_a^\infty \kappa_\perp d\kappa_\perp \left[1-\cos\left(\kappa_\perp^2 L\zeta^2 / k\right)\right] \times \exp\left[-\frac{1}{2}(\kappa_\perp L\zeta\theta)^2\right] \frac{\Phi_N(\kappa_\perp,0)}{\left[\kappa_\perp^2 v_\perp^2 - 4\pi^2 f^2\right]^{1/2}}$$

where $\Phi_N(\kappa_\perp,0) \propto \sigma_N^2(\zeta)\exp(-\kappa_\perp^2 l_0^2) L_0^{3-n}\kappa_\perp^{-n}$ is the spatial spectrum of electron density fluctuations;

$a = 2\pi f / v_\perp$, $\zeta = z/L$, $v_\perp \equiv v_\perp(\zeta) = v\sin\phi/(R(\zeta)/R_0)$, $\kappa_\perp = |\vec{\kappa}_\perp|$, $\vec{\kappa}_\perp = \{\kappa_x, \kappa_y\}$;

$\sigma_N^2(\zeta)$ is the dispersion of the relative electron density fluctuations $\delta N^2 / \langle N \rangle^2$;

L, L_0, l_0 are flow thickness, the outer and inner turbulence scales.

Analysis of spatial cross-correlation function

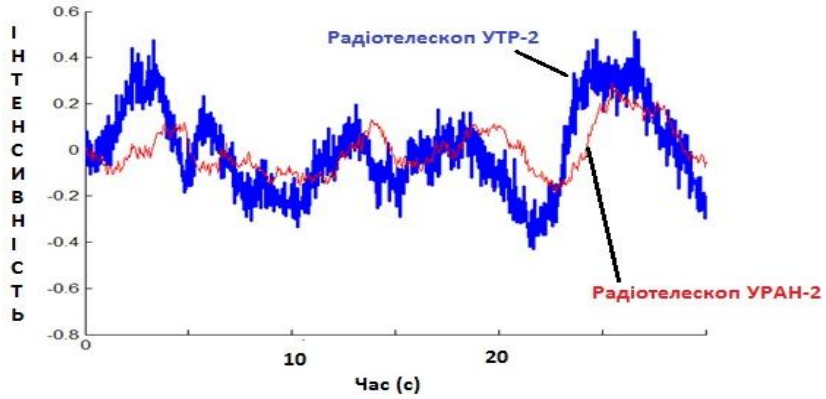

Figure 12. The synchronous records obtained with the radio telescopes UTR-2 (blue color) and URAN-2 (red color)

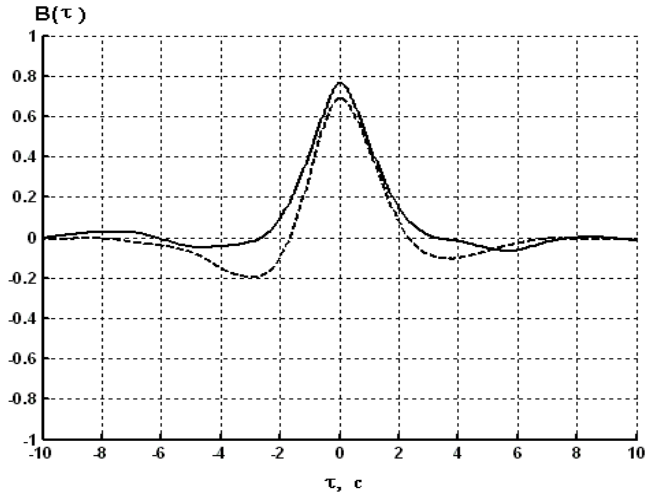

Figure 13. Cross-correlation function

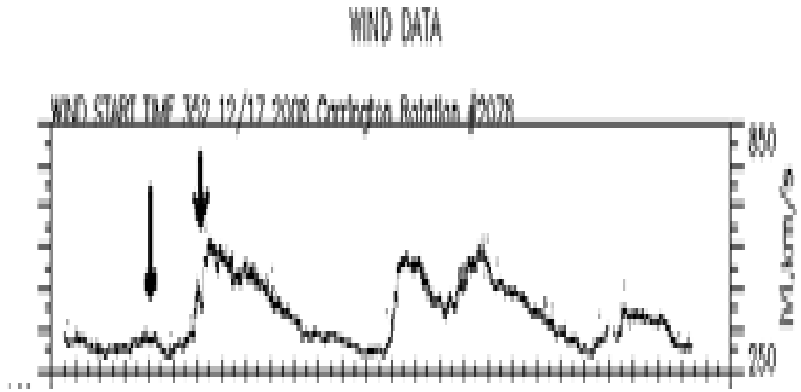

Figure 14. Solar wind velocity obtained by spacecraft “Wind”

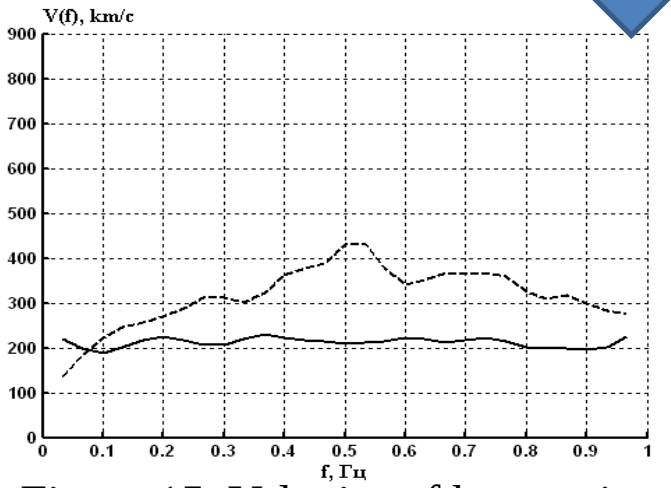

Figure 15. Velocity of harmonics of cross-spectrum

Spatial cross-correlation function analysis

The cross-correlation between scintillations in two points according to Feynman path integral technique

$$W(b,f) \approx \frac{\pi^2 I_0^2}{c^2\omega^2} \sum_{j=1}^{n} \int_0^1 d\zeta \int_{u_j}^{\infty} \kappa_\perp d\kappa_\perp \left\{ \frac{l_j \omega_{pj}^4}{\sqrt{\zeta}} \left[1-\cos\left(\kappa_\perp^2 \ell_j \zeta / k\right)\right] \times \right.$$

$$\left. \frac{\Phi_{Nj}(\kappa_\perp,0)\exp\left[2\pi i f b / v_{j\perp}(\zeta)\right]}{\left[\kappa_\perp^2 v_{j\perp}^2(\zeta) - 4\pi^2 f^2\right]^{1/2}} \right\} \exp\left[-\frac{1}{2}\kappa_\perp^2 L_n^2 \zeta^2 \theta^2\right]$$

The dispersion dependence

$$V(f) = {2\pi f b}\Big/{\Delta\varphi(f)}$$

where $\Delta\varphi(f) = arctg\left[{\mathrm{Im}W(b,f)}\Big/{\mathrm{Re}W(b,f)}\right]$

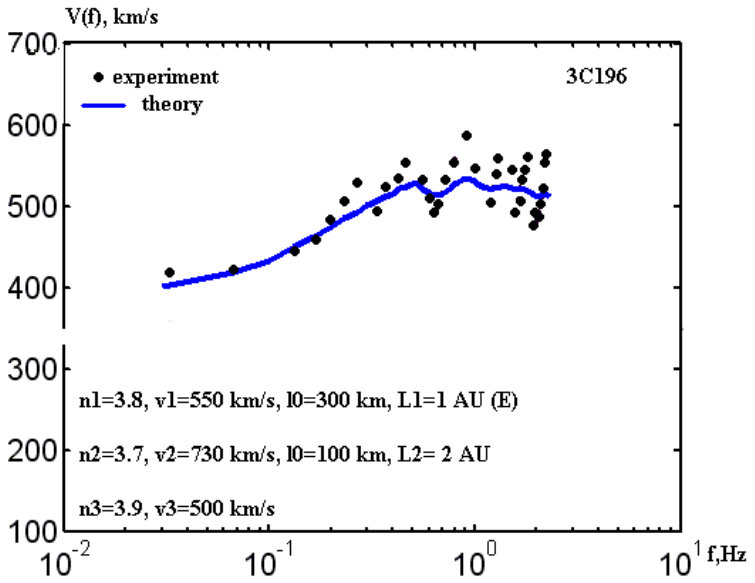

Figure 16. Example of model fitting.

The result of the reconstruction of the solar wind structure.

The case of one dense stream of the solar wind
which is situated close to the observer.

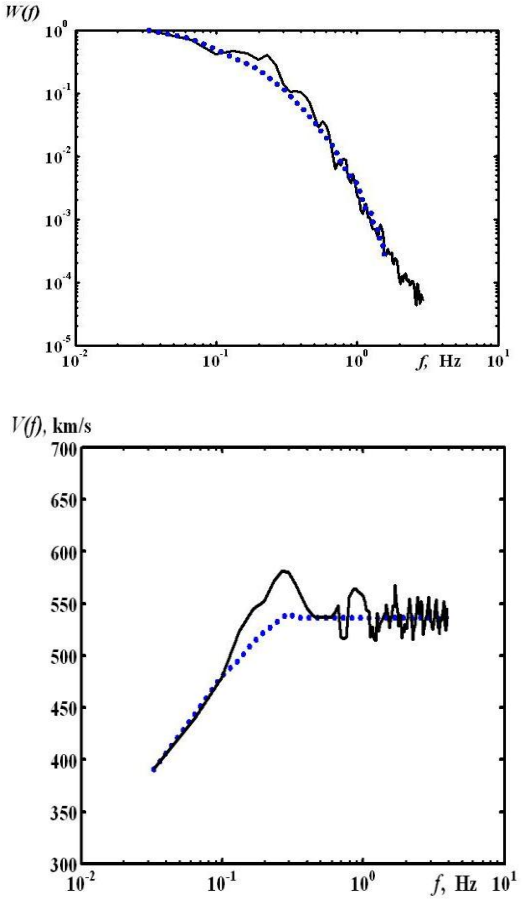

Figure 17. Model fitting theoretical to experimental IPS characteristics.

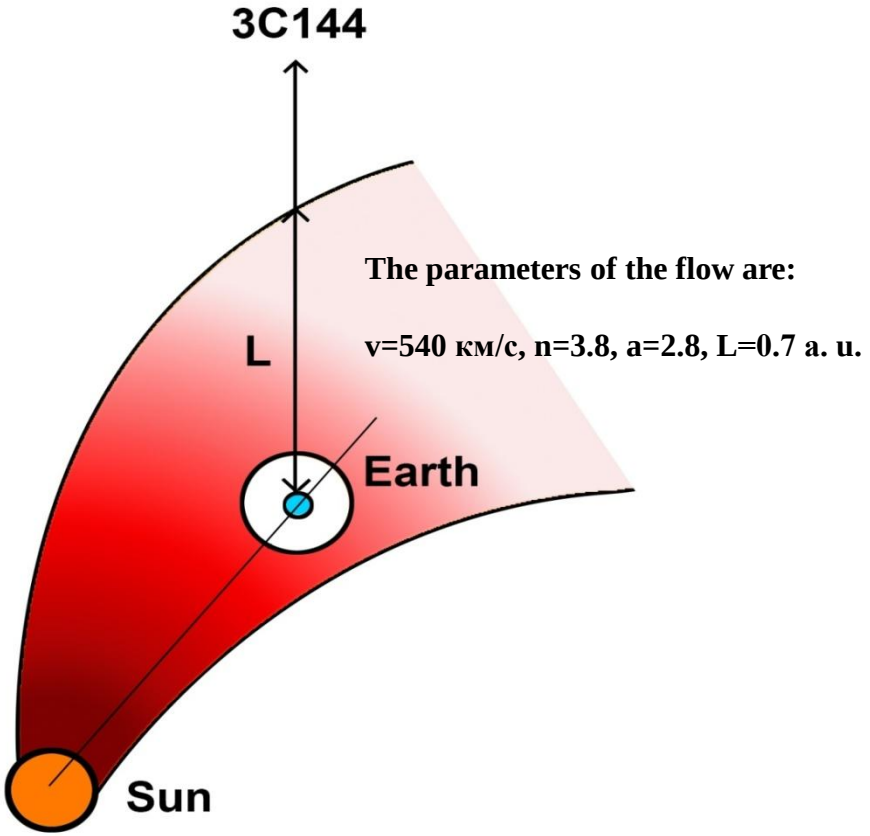

Figure 18. Model of the solar wind on the line of sight to the radio source 3C144 (2016.01.12).

Data obtained with the radio telescopes UTR-2 and URAN-2 .

The result of the reconstruction of the solar wind structure.

The case of three stream solar wind.

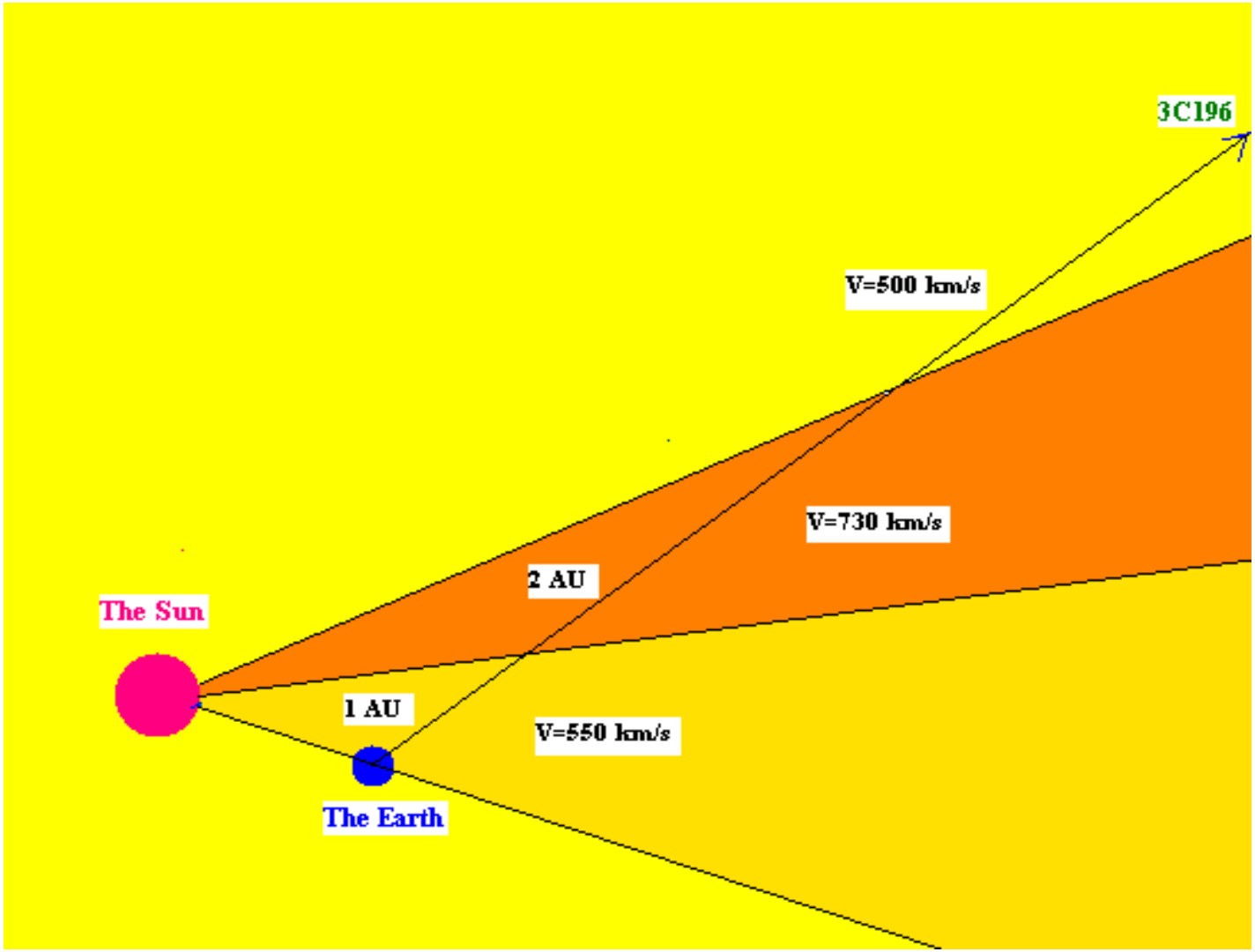

Figure 18. Radio source 3C196 (2013.10). Data obtained with the radio telescopes UTR-2 and URAN-2.

Example of IPS recording in case of ICME passing

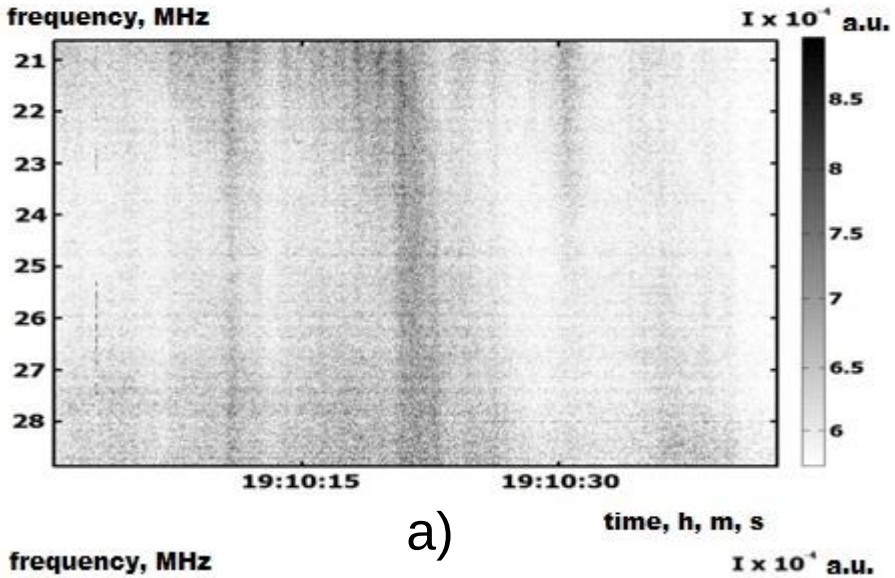

a)

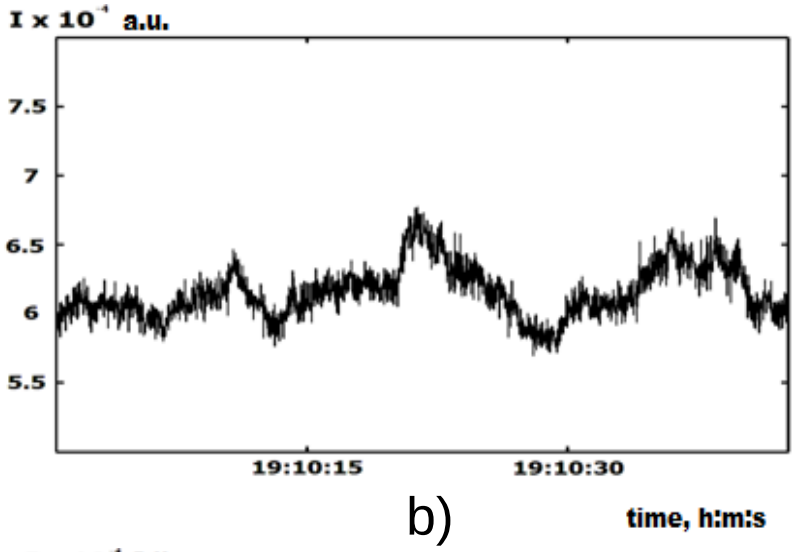

b)

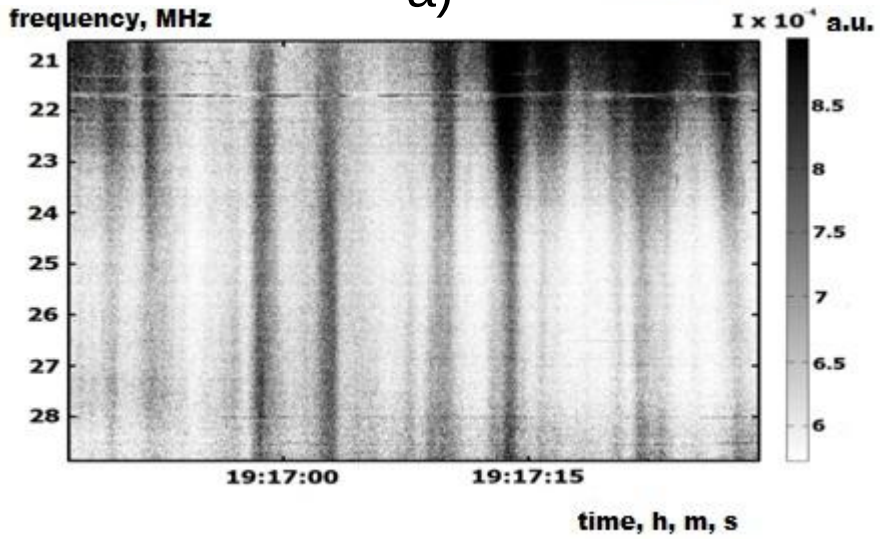

c)

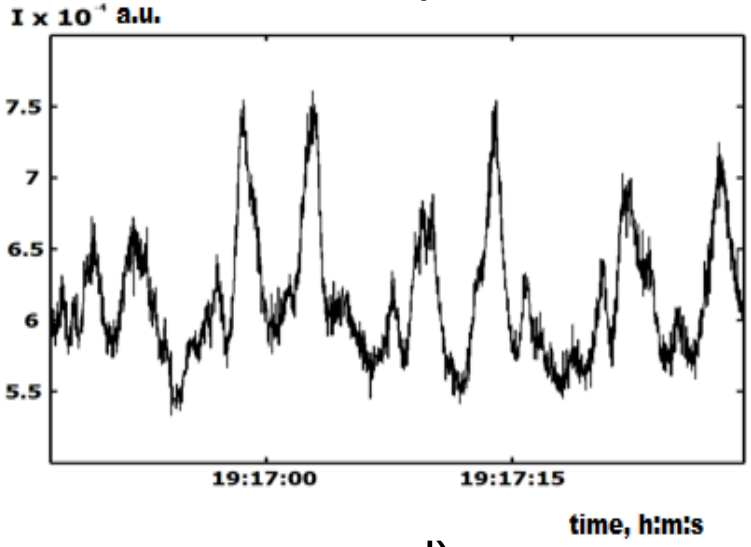

d)

Figure 19. Two examples of data recordings for ambient solar wind and when ICME passes the line of sight to the radio source. February 2011.

IPS characteristics in the case of ICME passing

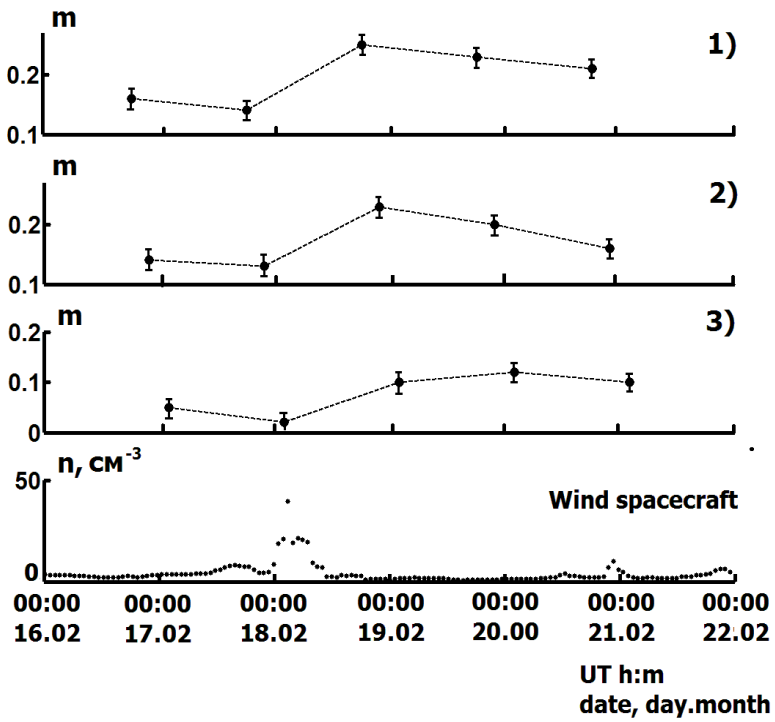

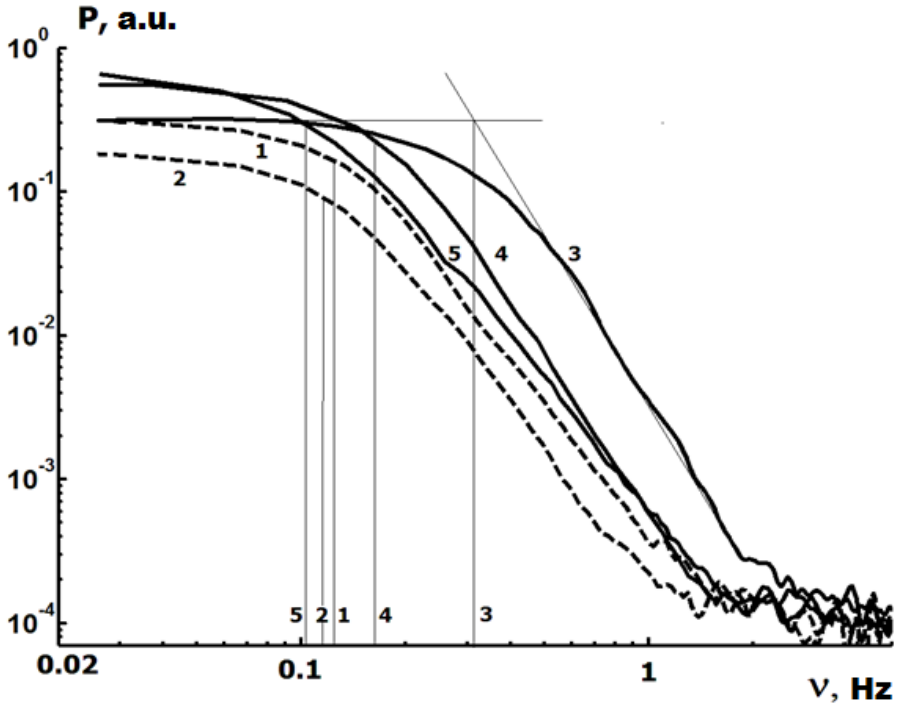

Figure 20. The behavior of the scintillation index and temporal intensity spectrum before and when ICME passes the line of sight to the radio radio source. February 2011.

The annual statistics of the velocities of slow(solid line) and fast (dashed line) solar wind streams for two years.

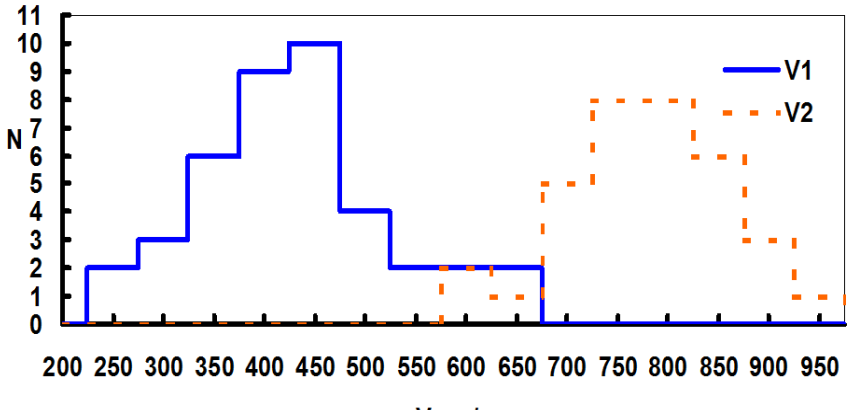

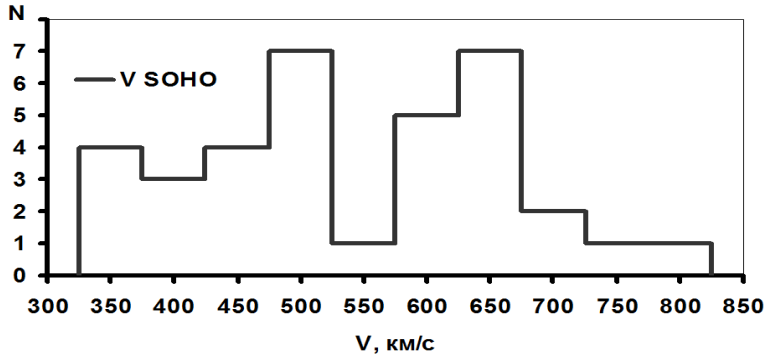

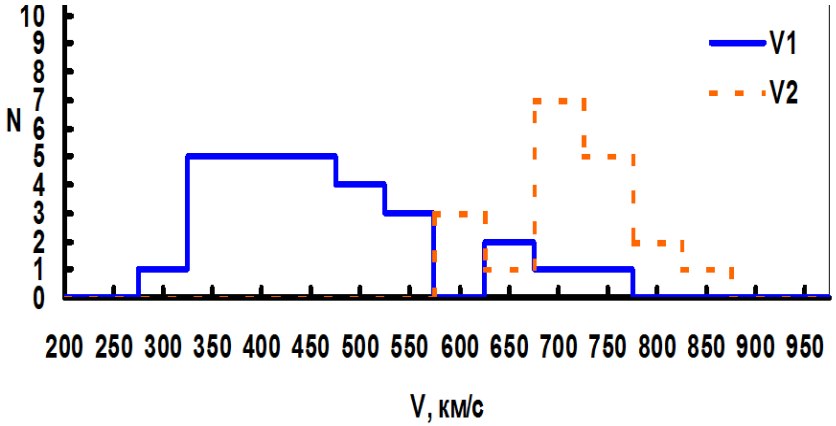

The annual statistics of the spectral index of the interplanetary turbulence spectra for two years.

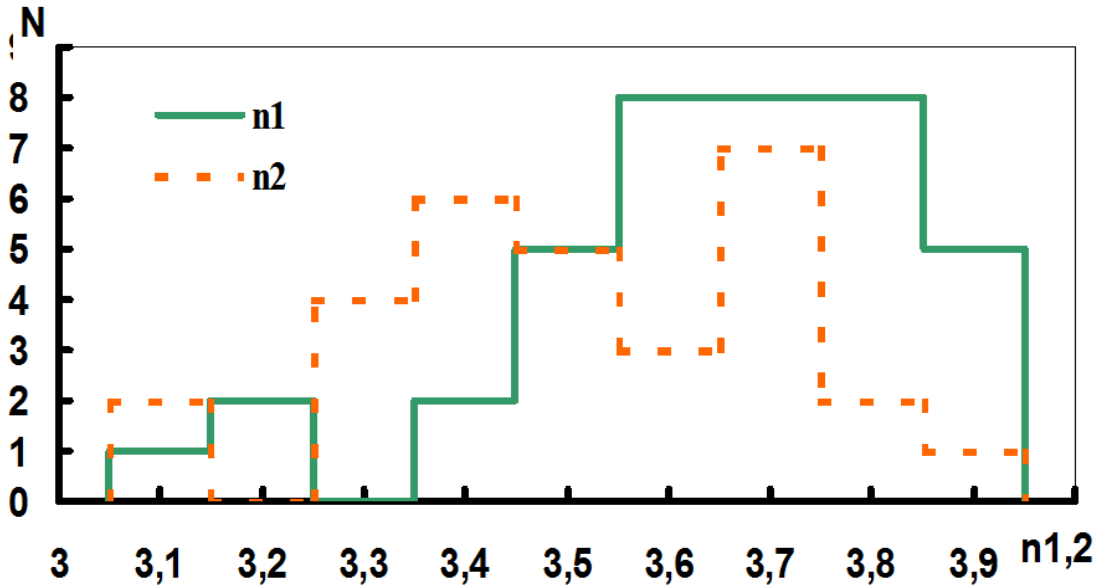

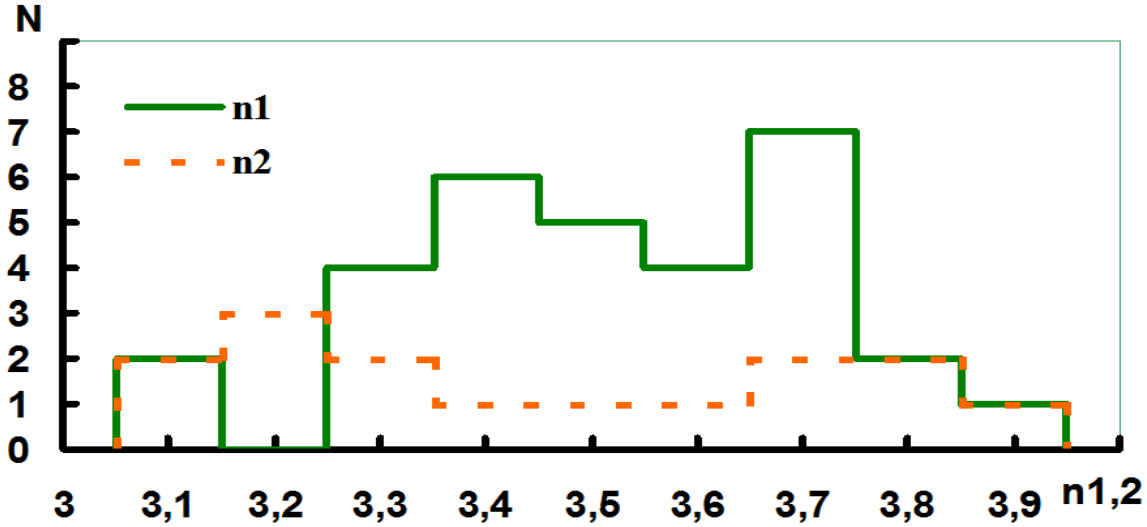

Perspectives

Creation of Giant Ukrainian Radio Telescopes (GURT).
(Frequency range 10 – 80 MHz). Gracove.

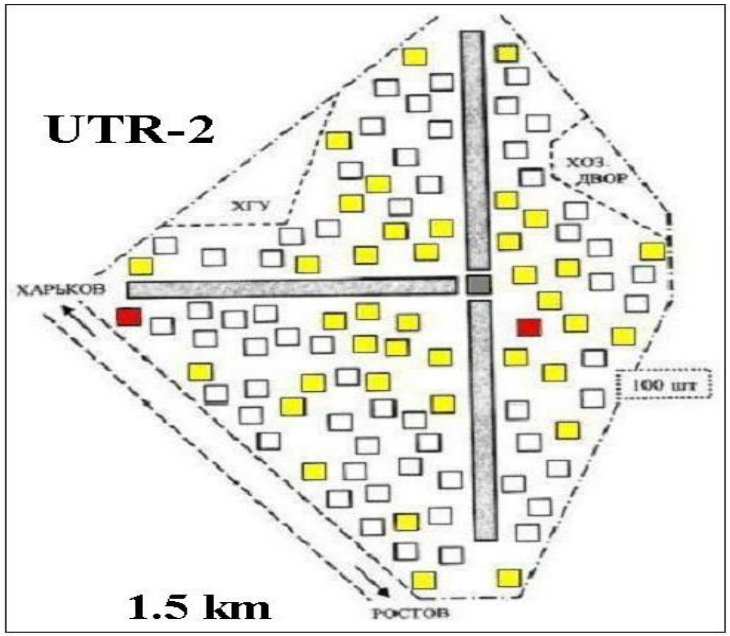

2 km

Radio telescope UTR-2 (T-shape)

and

Subarrays of Radio telescope GURT (squares)

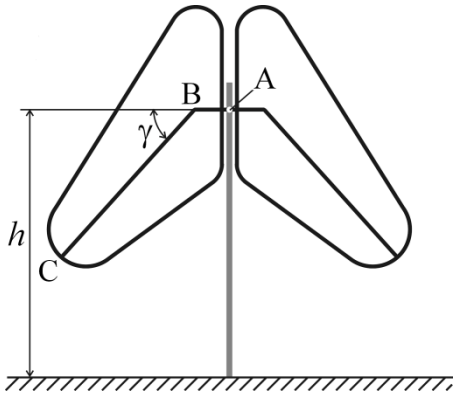

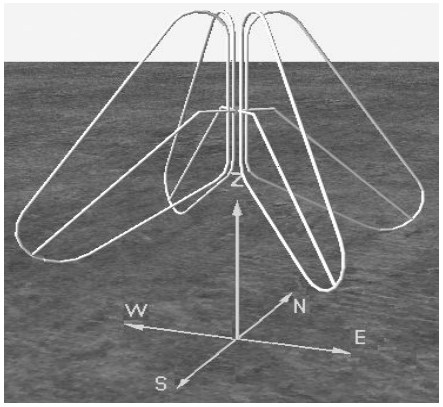

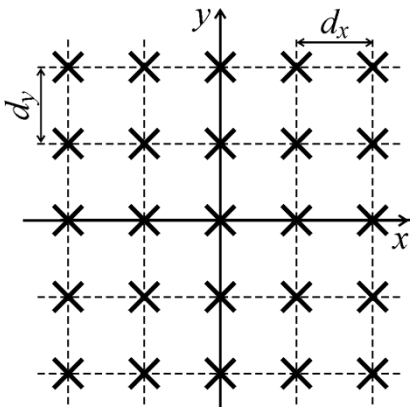

Creation of Giant Ukrainian Radio Telescopes (GURT).
(Frequency range 10 – 80 MHz)

Wide-band registration and data processing system

Fig. 23. The equipment room UTR-2 - GURT with back-end facilities of new generation.

Table New generation of broad-band digital spectral processors for UTR-2, URAN, and GURT.

Parameters	**DSPZ – UTR-2**	**ADR – GURT**
Frequency band (MHz)	8 – 32	8 – 80
Number of freq. channels	8 192	16 384
Frequency resolution (kHz)	4	5.450
Time resolution (msec)	0.5	0.183
ADC resolution (bits)	16	16
Dynamic range (dB)	90	90
Input channels	2	2
On-line real-time possibilities		
Fast Fourier transform	+	+
Waveform (non-limited duration)	+	+
Auto- and complex cross-correlation spectra	+	+
Sum-Subtraction mode	–	+
Signals normalization	–	+
Signals delay	–	+

Present state.

3 subarrays have been fully equipped. 6 subarrays have been partially equipped.

Fig. 24. UTR-2 and GURT radio telescope array.

Observations of IPS and IS with GURT

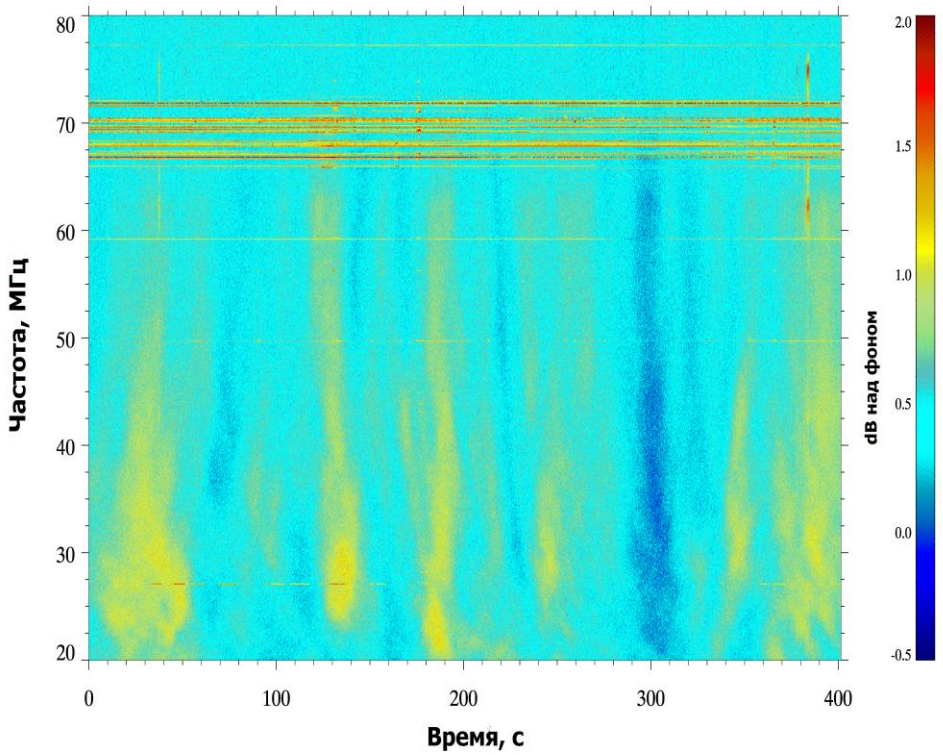

Fig. 26. The observations of the ionospheric scintillations of the radio source 3C461 (the radio telescope GURT)

Coordinated observations withUTR-2, URAN, LOFAR radio telescopes.

-Monitoring of interplanetary medium at distances from 0 to several a. u. by observations of IPS.

- Monitoring of Earth's ionosphere to find the reaction of it on active processes at the Sun

Conclusions

1. IPS observations at decameter wavelengths allow us to obtain the solar wind parameters and to reconstruct the stream structure of the solar wind on the line of sight to a radio source.
2. The new radio telescope GURT (10 – 80 MHz) enables us to rise the efficiency of such investigations especially at small solar elongations (less than 70 – 80 degrees).
3. Future plans for GURT are:

- synchronous observations of the solar radio bursts, IPS and IS with GURT – LOFAR- UTR-2 – URAN radio telescopes to study connections between the processes at the Sun, in the interplanetary and ionospheric plasma.

- Tracking the movement of ICME from the Sun to several a.u. to study their deceleration.

- Creation of reliable model of ICME movement for prediction of precise arrival time to Earth.

-……
- ……...

Thanks for attention